Two-Stage Atomic Layer Deposition of Aluminum Oxide on Alkanethiolate Self-Assembled Monolayers Using *n*-Propanol and Water as Oxygen Sources

Nobuhiko P. Kobayashi*,†,‡,§ and R. Stanley Williams‡

Jack Baskin School of Engineering, University of California Santa Cruz, Santa Cruz, California 95064, Information and Quantum Systems Laboratory, Hewlett-Packard Laboratories, Palo Alto, California 94304, and Nanostructured Energy Conversion Technology and Research (NECTAR), Advanced Studies Laboratories, University of California Santa Cruz and NASA Ames Research Center, Moffett Field, California 94035

Received October 3, 2007. Revised Manuscript Received April 28, 2008

Aluminum oxide (AlO_x) was deposited onto strong hydrophobic surfaces of alkanethiolate self-assembled monolayers (SAMs) by a two-stage atomic layer deposition (ALD) process; the first stage utilized *n*-propanol as the oxygen source, and the second stage proceeded with water. The resulting AlO_x layers were characterized with spectroscopic ellipsometry, reflection−absorption infrared spectroscopy, low-energy X-ray emission spectroscopy, and atomic force microscopy. The optimized two-step ALD process significantly improved the surface morphology of AlO_x layers and effectively protected the structural integrities of underlying SAMs.

Introduction

In electronic devices based on molecular layers, inorganic encapsulation layers are often utilized to effectively protect and electrically gate the organic molecules.[1,2] Apart from encapsulation for electronic devices, conducting metal oxides of titanium and molybdenum directly contacted to an organic layer in a light-emitting diode structure have been reported to improve air stability performance.[3] In the development of such an inorganic encapsulation, inorganic films such as aluminum oxide were deposited and studied on various types of self-assembled monolayers (SAMs). For instance, the deposition of aluminum oxide has been studied on hydrophobic hydroxyl-terminated SAMs using metal organic chemical vapor deposition to demonstrate the construction of superstructures of alternating organic/inorganic layers.[4] In addition to binary oxides, deposition characteristics of other inorganic layers such as metals and nitrides have also been extensively studied. Titanium, magnesium, copper, and calcium were deposited on SAMs terminated with various terminal groups including $-CH_3$, $-COOH$, $-OH$, OCH_3, and $-CO_2CH_3$,[5–7] and gold deposition was studied on a thiolated surface.[8] Effects of interfacial organic layers on thin film nucleation in atomic layer deposition (ALD) of titanium nitrides revealed that the initial rate of growth was strongly attenuated and the film morphologies were severely islanded on SAMs with nonreactive $-CH_3$ end groups.[9,10]

We previously studied the evolution of aluminum oxide (AlO_x) deposited on hydrophobic and hydrophilic surfaces by ALD with water as an oxygen source.[11] The AlO_x layers deposited on hydrophobic surfaces developed extremely rough surface morphologies while those deposited on hydrophilic surfaces displayed minimal kinetic roughening. The considerable differences in the surface morphology of AlO_x deposited on hydrophobic and hydrophilic surfaces were attributed to their surface wettability by water. Therefore, we suggested the importance of explicitly controlling surface wettability in the early stages of ALD, in particular, for strong hydrophobic surfaces. In this paper, we describe a two-stage process for nucleating and growing smoother AlO_x layers on strong hydrophobic alkanethiolate SAMs that also maintain the structural integrities of the molecular layer even after the deposition of AlO_x.

Experimental Section

An ALD apparatus used in the experiment consists of a stainless steel reaction chamber that can accommodate a 4-in. wafer. The chamber is equipped with a dry pump that maintains the chamber base pressure $\sim 1 \times 10^{-3}$ torr. Three precursors, trimethylaluminum (aluminum source), water, and *n*-propanol (oxygen sources), for

* Corresponding author. E-mail: nobby@soe.ucsc.edu. Phone: 831-459-3571.
† University of California Santa Cruz.
‡ Hewlett-Packard Laboratories.
§ NECTAR/Advanced Studies Laboratories, UCSC - NASA ARC.

(1) Dimitrakopoulos, C. D.; Mascaro, D. J. *IBM J. Res. Dev.* **2001**, *45*, 11.
(2) Toniolo, R.; U Hmmelgen, I. A. *Macromol. Mater. Eng.* **2004**, *289*, 311.
(3) Morii, K.; Ishida, M.; Takashima, T.; Shimoda, T.; Wang, Q.; Nazeeruddin, Mh. K.; Grätzel, M. *Appl. Phys. Lett.* **2006**, *89*, 183510.
(4) Wohlfart, P.; Weiss, J.; Käshammer, J.; Kreiter, M.; Winter, C.; Fisher, R.; Mittler-Neher, S. *Chem. Vap. Deposition* **1999**, *5*, 165.
(5) Nagy, G.; Walker, A. V. *J. Phys. Chem. C* **2007**, *111*, 8543.
(6) Walker, A. V.; Tighe, T. B.; C Haynie, B.; Uppili, S.; Winograd, N.; Allara, D. L. *J. Phys. Chem. B* **2005**, *109*, 11263.
(7) Nagy, G.; Walker, A. V. *J Phys. Chem. B* **2006**, *110*, 12543.
(8) Käshammer, J.; Wohlfart, P.; Weiss, J.; Winter, C.; Fisher, R.; Mittler-Heher, S. *Opt. Mater.* **1998**, *9*, 406.
(9) Dube, A.; Sharma, M.; Ma, P. F.; Engstrom, J. R. *Appl. Phys. Lett.* **2006**, *89*, 164108.
(10) Dube, A.; Sharma, M.; Ma, P. F.; Ercius, P. A.; Muller, D. A.; Engstrom, J. R. *J. Phys. Chem. C* **2007**, *111*, 11045.
(11) Kobayashi, N. P.; Donley, C. L.; Wang, S.-Y.; Williams, R. S. *J. Cryst. Growth* **2007**, *299*, 218.

10.1021/cm702848y CCC: $40.75
Published on Web 07/30/2008

the deposition of AlO_x, are stored in three separated stainless steel cylinders with a hand valve and kept at room temperature. Each precursor assembly is connected to one of the four inlets of a mixing gas chamber assembled with three high-speed solenoid valves. The fourth inlet is connected to a source of high-purity nitrogen carrier gas and the outlet of the mixing gas chamber is connected to the reaction chamber. Each precursor is picked up by the nitrogen carrier gas and injected into the reaction chamber when an associated high-speed solenoid valve is opened. During an ALD run, the nitrogen carrier gas flows through the reaction chamber continuously even when no precursor is injected. Since trimethylaluminum is pyrophoric, care should be taken to ensure that the entire apparatus is leak tight using appropriate leak-check techniques. A wafer in the reaction chamber is heated up with a resistive heater. All ALD process parameters such as the wafer temperature and the operation sequence of the high-speed solenoid valves are controlled by a computer.

The samples used in this study were prepared as follows. A gold film with an atomically smooth surface was first prepared by template stripping (TS-gold)[12] on a glass substrate. Subsequently, the gold film was covered by a SAM of CH_3-terminated alkanethiolate ($CH_3-(CH_2)_{17}-SH$) to obtain a strong hydrophobic surface on which an AlO_x layer was deposited by ALD. Complete details of the preparation process of the CH_3-terminated SAM (CH_3-SAM) on an atomically smooth gold film were reported previously.[11] On the CH_3-SAM, the formation of water droplets during ALD of AlO_x using water as an oxygen source was postulated to be the cause of the observed growth instability, leading to substantially rough surface morphologies of AlO_x.[11] Therefore, we attempted to explicitly control the surface wettability on the CH_3-SAM by utilizing *n*-propanol, instead of water, as an oxygen source in the early stage of an ALD run, that is, a two-stage ALD process in which the first stage utilizes *n*-propanol as the oxygen source and the second stage proceeds with water. *n*-Propanol and water exhibit comparable physical properties, for instance, the vapor pressure of *n*-propanol at 25 °C is ~21.1 mmHg, compatible to that of water (~23.8 mmHg), and the heat of vaporization for *n*-propanol and water are 47.5 and 40.7 kJ/mol, respectively.[13]

The resulting AlO_x layers were characterized with spectroscopic ellipsometry, reflection−absorption infrared spectroscopy (RAIRS), low-energy X-ray emission spectroscopy (LEXES), and atomic force microscopy (AFM). With these complementary characterization tools, the two-stage ALD process was optimized in terms of surface morphologies of AlO_x layers and structural integrities of underlying CH_3-SAMs. The spectroscopic ellipsometer is equipped with three lasers with wavelengths at 543.5, 632.8, and 832.2 nm. Both an incident and an exit angle of the laser optical axis with respect to the surface normal of a sample are fixed to 70°. RAIRS measurement was carried out with FTIR (Nicolet Nexus 870 FTIR) equipped with a RAIRS set up with incident and exit glancing angles of 80° with respect to the surface normal of a sample. A TS−gold sample not covered with SAMs was used as a reference to obtain absorbance. In LEXES analysis, an energetic electron beam at 0.5 keV was used to irradiate the samples. The primary electron beam creates core-level vacancies in the atoms, and de-excitation occurs when an electron from a higher orbital drops into the vacated hole and emits a characteristic X-ray photon. The emitted X-rays are analyzed using wavelength dispersive spectrometers (WDS) to obtain quantitative elemental information. AFM was operated in tapping mode with a silicon cantilever.

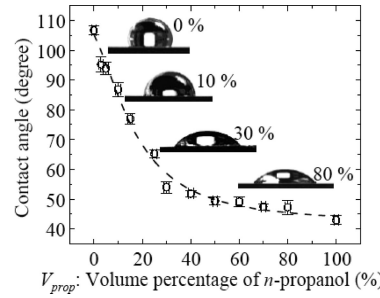

Figure 1. Contact angles measured on a CH_3-SAM layer using a mixture of water and *n*-propanol with various concentrations of *n*-propanol. Four representative images of a droplet of the various mixtures from which the contact angles were obtained are also displayed as insets.

Results

Plotted in Figure 1 are contact angles measured on a CH_3-SAM using various mixtures of water and *n*-propanol as a function of the volume percentage of *n*-propanol in the mixture (V_{prop}). Also in Figure 1 are the four images collected during the contact angle measurement representing a side view of liquid droplets of a mixture of $V_{prop} = 0$, 10, 30, and 80% as denoted. The contact angle monotonically decreased until V_{prop} reached ~30%, and then, it saturated at ~45°, suggesting that the surface wetting on strong hydrophobic CH_3-SAM surfaces is expected to improve if *n*-propanol, instead of water, is used in the early stage of the ALD process of AlO_x. Therefore, we proposed the two-stage ALD process as described in the previous section. We utilized pure *n*-propanol held at 25 °C as the oxygen source in the first stage to initiate uniform nucleation of AlO_x on the CH_3-SAM, employing the better wettability of *n*-propanol on the CH_3-SAM as suggested in Figure 1. Subsequently, in the second stage, water held at 25 °C was used as the oxygen source to further deposit AlO_x on the surface of AlO_x deposited in the first stage. In both deposition stages, trimethylaluminum (TMAl) held at 25 °C was used as the aluminum source. One ALD cycle in the first stage was performed by supplying a 140 ms *n*-propanol pulse, a 160 s nitrogen purge period, a 140 ms TMAl pulse, and a 16 s nitrogen purge period. In the second stage, one cycle was performed in the same sequence as in the first stage using water instead of *n*-propanol. These specific deposition conditions were calibrated for AlO_x on OH-terminated silicon surfaces at 45 °C to maintain deposition rates self-limited at 0.014 and 0.077 nm/cycle in an *n*-propanol and a water ALD stage, respectively.

All samples described below are identified by the cycle fraction $R_c = N_{n\text{-propanol}}/(N_{n\text{-propanol}} + N_{water})$, where $N_{n\text{-propanol}}$ and N_{water} are the total number of ALD cycles in an *n*-propanol (the first stage) and a water stage (the second stage), respectively. The substrate temperature was set to 45 °C for all samples to minimize structural damage associated with thermal effects on the CH_3-SAMs.[14] The total number of pulses used in a deposition process was adjusted for a given R_c to produce the same total layer thickness for all samples; thus, nominal thicknesses of the

(12) Blackstock, J. J.; Li, Z.; Freeman, M. R.; Stewart, D. R. *Surf. Sci.* **2003**, *546*, 87.
(13) http://webbook.nist.gov/chemistry/name-ser.html (Accessed June 2008).
(14) Prathima, N.; Harini, M.; Rai, N.; Chandrashekara, R. H.; Ayappa, K. G.; Sampath, S.; Biswas, S. K. *Langmuir* **2005**, *21*, 2364.

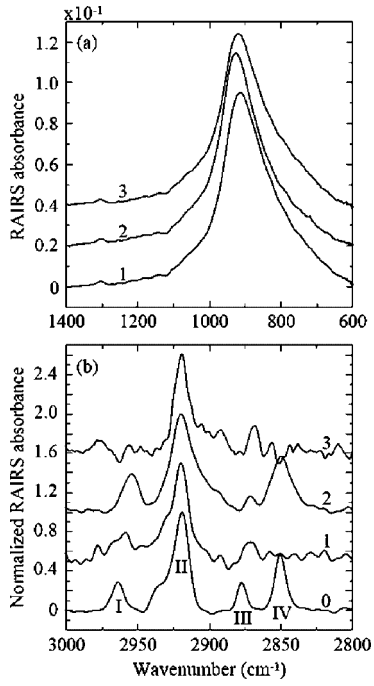

Figure 2. RAIRS spectra collected from the $R_c = 0.002$ (spectrum 1), $R_c = 0.301$ (spectrum 2), and $R_c = 0.826$ (spectrum 3) samples. Peaks associated with several overlapping Al−O stretching modes are presented in (a). Panel (b) shows four peaks, labeled as I, II, III, and IV, associated with C−H stretching modes of the CH_3−SAMs underneath the AlO_x layers. Spectrum 0 on the bottom represents a spectrum collected from an as-formed CH_3−SAM.

Table 1. LEXES Results Showing Carbon, Aluminum, and Oxygen Contents in the AlO_x Layers with Different R_c

R_c	C (atom %)	Al (atom %)	O (atom %)
0.002	5.7	35.4	57.2
0.064	6.5	35.8	57.2
0.151	7.9	35.2	56.8
0.301	7.6	35.2	57.2

AlO_x layers measured by spectroscopic ellipsometry were within 31 ± 1 nm on all samples regardless of R_c.

Figure 2a,b shows RAIRS data collected from $R_c = 0.002$ (spectrum 1), $R_c = 0.301$ (spectrum 2), and $R_c = 0.826$ (spectrum 3) samples. RAIRS peaks associated with several overlapping Al−O modes are presented in panel a. In panel a, the spectra 2 and 3 are shifted upward (i.e., along the RAIRS absorbance axis) by 0.2×10^{-1} and 0.4×10^{-1} for the ease of view. The three spectra are nearly identical in terms of both their peak absorbance and shapes, suggesting that the overall chemical and physical characteristics of the AlO_x layers deposited with various R_c are comparable. In addition to the RAIRS data, chemical compositions of the AlO_x layers were obtained by LEXES, which effectively integrates over the entire AlO_x layer thickness, collected from witness samples deposited on OH-terminated silicon surfaces, and shown in Table 1. The elemental compositions were nearly comparable for all samples except for the gradual increase seen in carbon content as R_c increased.

Figure 2b displays RAIRS spectra associated with the CH_3−SAM underneath the AlO_x layers. The three spectra represent $R_c = 0.002$ (spectrum 1), $R_c = 0.301$ (spectrum 2), and $R_c = 0.826$ (spectrum 3). The spectrum 0 on the bottom was collected from an as-formed CH_3−SAM with no AlO_x overlayer and is shown as a reference. The four peaks marked I, II, III, and IV are associated with asymmetric CH_3, asymmetric CH_2, symmetric CH_3, and symmetric CH_2 stretching modes, respectively.[15] Since the absolute absorbance of each peak is highly sensitive to total structural characteristics of each sample, the absorption peaks of each spectrum were normalized with respect to the absorbance of the asymmetric CH_2 peak (i.e., peak II) of each spectrum. The spectra 1, 2, and 3 are shifted upward (i.e., along the axis of normalized RAIRS absorbance) for the ease of view. Table 2 summarizes the peak wavenumbers for each spectrum.

Table 2. RAIRS Peak Positions Associated with C−H Stretching Modes of the CH_3−SAMs for the Four Characteristic Peaks I, II, III, and IV As Marked for Sepctrom 0 in Figure 2b

	peak (cm^{-1})			
spectrum	I	II	III	IV
3	no peak	2919.6	2867.6	no peak
2	2954.4	1919.6	2872.4	2849.3
1	2959.2	2919.6	2871.4	no peak
0	2964	2918.7	2877.2	2850.2

For the $R_c = 0.301$ sample (spectrum 2), the four characteristic peaks resolved clearly indicate that the chemical and structural integrities of the as-formed CH_3−SAM (spectrum 0) were well preserved even after the deposition of AlO_x. In spectrum 2, the peak positions of peaks II and IV revealed no discernible peak shift with respect to the corresponding peak positions for the as-formed CH_3−SAM, which further indicates that the alkyl chains were still well-ordered. A broadened shoulder on the lower wavenumber side of peak II is an indication of slight mode-softening within the alkyl chains.[16] The positions of peaks I (2954.4 cm^{-1}) and III (2849.3 cm^{-1}) were shifted toward lower wavenumbers compared to those for the as-formed CH_3−SAM (2964.1 and 2850.3 cm^{-1}), which also indicates slight mode-softening of the terminal methyl groups.[17]

In contrast to the spectrum of the $R_c = 0.301$ sample (spectrum 2), the spectra of the $R_c = 0.002$ (a single *n*-propanol ALD cycle followed by a 400-cycle water stage, spectrum 1) and 0.826 (spectrum 3) samples revealed that all the vibration modes were severely perturbed by the AlO_x deposition. In both spectra, although peak II was still present, peak IV was completely absent, which could be attributed to symmetry-breaking in the alkyl chains.[18] Furthermore, peak I appeared to consist of multiple small peaks, in particular in spectrum 1, suggesting the presence of both in-plane and out-of-plane asymmetric vibrational modes of CH_3. In addition, for the $R_c = 0.002$ sample (spectrum 1), the characteristics of RAIRS peaks were consistent with our previous observations on the AlO_x deposition with water only (note: more than 99% of ALD cycles were carried out with water for the $R_c = 0.002$ sample; thus, this sample was effectively identical to a sample deposited with water only as described in our previous paper[11]).

(15) MacPhail, R. A.; Strauss, H. L.; Snyder, R. G.; Elliger, C. A. *J. Phys. Chem.* **1984**, *88*, 334.
(16) Hostetler, M. J.; Manner, W. L.; Nuzzo, R. G.; Girolami, G. S. *J. Phys. Chem.* **1995**, *99*, 15269.
(17) Michaelides, A.; Hu, P. *J. Chem. Phys.* **2001**, *114*, 2523.
(18) Yamamoto, M.; Sakurai, Y.; Hosoi, Y.; IshiiH.; Ito, E.; Kajikawa, K.; Ouchi, Y.; Seki; K., K. *Surf. Sci.* **1999**, *427−428*, 388.

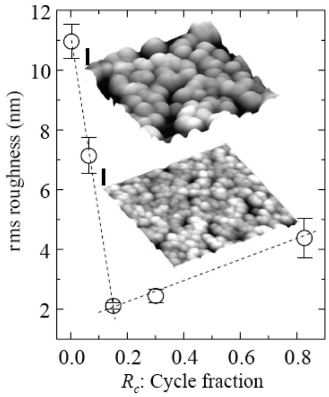

Figure 3. Root-mean-square roughness obtained by AFM for the AlO_x samples with various R_c. AFM images collected on the AlO_x samples with $R_c = 0.002$ (top) and 0.301 (bottom) are shown as insets. Each image represents a 500 × 500 nm scan, and the vertical scale bar corresponds to 60 nm.

Plotted in Figure 3 are root-mean-square (rms) roughness data collected on the AlO_x layers with various R_c using AFM, revealing the presence of a window of $R_c \sim 0.2$ within which the rms roughness was minimized. Beyond the $R_c \sim 0.2$ window, the rms roughness appeared to increase as R_c increased. Shown as insets in Figure 3 are representative AFM images (500 nm × 500 nm scan) collected from the AlO_x samples with $R_c = 0.002$ (11 nm rms roughness) on the top and $R_c = 0.301$ (2.4 nm rms roughness) on the bottom, showing characteristic granular features on two different surfaces. The granular features on the $R_c = 0.301$ sample (bottom) were much finer in both vertical and lateral extensions than those on the $R_c = 0.002$ sample (top).

Discussion

Conventional ALD processes for a binary alloy proceed by alternatively providing a pulse of a precursor that contains one of two constituents. Each precursor pulse is separated by a period in which an inert gas pulse is provided to ensure that the surface is saturated with a monolayer of one of the two precursors (i.e., self-limiting surface reactions).[19] Atomistic ALD mechanisms have been theoretically investigated by density functional theories.[20,21] Experimentally, on hydrogen-terminated silicon surfaces, an incubation period was observed at the beginning of the ALD process with trimethylaluminum and water, and the observed incubation period was attributed to the time required for the formation of interfacial silicon suboxide.[22,23] A study on the correlation between ALD cycles and surface hydroxyl group concentrations in AlO_x ALD processes revealed that steric hindrance by adsorbed methyl groups terminated the trimethylaluminum reaction.[24]

The two-stage ALD process for AlO_x with $R_c \sim 0.2$ produced superior results on strong hydrophobic CH_3−SAM surfaces in terms of resulting surface morphologies of the AlO_x and structural integreties of the underlying CH_3−SAMs, showing marked contrast to conventional ALD processes that use water as a sole oxygen source on strong hydrophobic surfaces. As indicated in Figure 1, the wettability on the CH_3−SAM surfaces was expected to improve substantially when pure *n*-propanol was used as the oxygen source, which consequently resulted in significant improvement in the surface morphologies of AlO_x. This proved that our original hypothesis that explicitly controlling the surface wetting in the early stage of ALD process is critical to obtain AlO_x layers with smooth surface morphologies was correct.[11]

Characteristics of the AlO_x layers deposited by the two-stage ALD process were assessed by analyzing Figure 2a. The three spectra 1, 2, and 3 associated with overlapping Al−O vibrational modes indicate overall chemical characteristics of the three AlO_x layers deposited with various R_c are comparable in relation to their shapes, peak wavenumbers, and peak absorbance. AlO_x formed at a relatively low temperature is composed mainly of γ-Al_2O_3. Since the Al−O vibrational mode peaks of γ-Al_2O_3 shown in Figure 2a are mainly associated with the surface phonon mode of alumina, a slight shift toward higher wavenumber observed at the peak position of spectrum 2 in comparison to those of spectra 1 and 3 suggests that the granular features existing on the surface of $R_c = 0.301$ (spectrum 2) sample are much finer than those on the $R_c = 0.002$ (spectrum 1) and $R_c = 0.826$ (spectrum 3) samples.[25] The presence of finer granular features on the $R_c = 0.301$ sample is further supported by the AFM image shown in the bottom inset of Figure 3 and certainly contributes to the improved surface morphology for the $R_c = 0.301$ sample.

The core result is summarized as follows. In the two-stage ALD of AlO_x on strong hydrophobic CH_3−SAM surfaces, rms roughness of the AlO_x can be minimized and structural integrities of the CH_3−SAMs can be maintained within the narrow window of $R_c \sim 0.2$. As shown in Figure 3, the rms roughness dropped rapidly as R_c increased toward 0.2 in the smaller R_c ($R_c < 0.2$) range, which suggests that, given the improved wettability on CH_3−SAM surfaces with *n*-propanol used in the first stage, the rms roughness of AlO_x layers deposited in the second stage improves as the surface coverage (on the CH_3−SAM surfaces) of the AlO_x deposited in the first stage increases (i.e., R_c increases). In other words, once nearly an entire CH_3−SAM surface is covered with AlO_x in the first stage (i.e., at $R_c \sim 0.2$), a subsequent AlO_x deposition in the second stage with water proceeds with a smooth surface morphology because the deposition in the second stage is carried out on a hydrophilic AlO_x surface prepared in the first stage.

Figure 3 also shows that the rms roughness appears to increase gradually beyond $R_c \sim 0.2$, which could be explained as follows. As R_c increases, the thickness of AlO_x deposited with *n*-propanol in the first stage increases; that is, the thickness of AlO_x deposited with water in the second

(19) Ott, A. W.; Klaus, J. W.; Johnson, J. M.; George, S. M. *Thin Solid Films* **1997**, *292*, 135.
(20) Widjaja, Y.; Musgrave, C. B. *Appl. Phys. Lett.* **2002**, *80*, 3304.
(21) Halls, M. D.; Raghavachari, K. *J. Chem. Phys.* **2003**, *118*, 10221.
(22) Busch, B. W.; Pluchery, O.; Chabal, Y. J.; Muller, D. A.; Opila, R. L.; Kwo, J. R.; Garfunkel, E. *MRS Bull.* **2002**, *27*, 206.
(23) Gosset, L. G.; Damlencourt, J. F.; Renault, O.; Rouchon, D.; Holliger, P.; Ermolieff, A.; Trimaille, I.; Ganem, J. J.; Martin, F.; Semeria, M. N. *J. Non-Cryst. Solids* **2002**, *80*, 4241.
(24) Puurunen, R. L. *Appl. Surf. Sci.* **2005**, *245*, 6.
(25) Ying, J. Y.; Benziger, J. B.; Gleiter, H. *Phys. Rev. B* **1993**, *48*, 1830.

stage decreases (note that the nominal total thickness for all samples is 31 nm regardless R_c); therefore, the increase in the carbon content indicated by the LEXES data in Table 1 can be attributed to the increase in the thickness of AlO_x deposited in the first stage with *n*-propanol. In the second stage, wettability with water on the AlO_x surface prepared in the first stage would degrade as the total amount of carbon in the AlO_x deposited in the first stage increases (i.e., R_c increases beyond 0.2), which would account for the gradual increase in the rms roughness beyond $R_c \sim 0.2$ in Figure 3. We performed contact angle measurements on a 14 nm thick AlO_x layer deposited only with *n*-propanol (i.e., an AlO_x layer expected to contain ~8.2 atom % of carbon, which corresponds to the $R_c = 0.826$ sample after the first stage is completed) and found that the contact angle for water was 29.4°, which is approximately 50% higher than those measured on an AlO_x layer deposited only with water (i.e., an AlO_x layer expected to contain much less carbon). This suggests that the wettability of water on a thick AlO_x, as in the $R_c = 0.826$ sample, deposited with *n*-propanol degrades. In other words, the AlO_x surfaces would roughen in the larger R_c ($R_c > 0.2$) range because of the degraded wettability on an AlO_x surface prepared in the first stage with a large R_c, resulting in the appearance of the narrow R_c window in Figure 3 within which the rms roughness is minimized.

A major unanticipated bonus was that the CH_3-SAM was much less perturbed by the two-stage AlO_x ALD as shown by the RAIRS spectrum in Figure 2b for the $R_c = 0.301$ sample (spectrum 2). Severe disruption on the CH_3-SAM for the $R_c = 0.002$ (spectrum 1) in Figure 2b is consistent with the results for the CH_3-SAM covered by an ALD AlO_x layer deposited by a conventional ALD process with water;[11] therefore, in the smaller R_c range ($R_c < 0.2$), an incomplete AlO_x layer deposited in the first stage is not able to protect an underlying CH_3-SAM from chemically harsh pyrophoric reactions between water and trimethylaluminum when the deposition is switched to the second stage.

Addressing the mechanisms that would have caused the severe disruption in the CH_3-SAMs as seen in spectrum 3 in Figure 2b for the $R_c = 0.826$ sample would need to invoke several different contributions. First, throughout the first stage required for the $R_c = 0.826$ sample, the CH_3-SAM is exposed to *n*-propanol for an extended period of time. Alcohol such as *n*-propanol has a capability to chemically attack alkane chains in CH_3-SAMs when the SAMs are exposed to alcohol for a prolonged time period.[26] During the long period of time required for $R_c = 0.826$ sample in the first stage, the CH_3-SAM is exposed to *n*-propanol repeatedly, which would cause substantial structural damages on its alkane chains. A significant contribution to the disruption of the underlying CH_3-SAM can also be associated with mechanical strain generated by a roughening AlO_x layer, which can account for the disruption of CH_3-SAMs for both $R_c = 0.002$ and 0.826 samples. In both samples, as the AlO_x layer on the CH_3-SAM surface roughens, substantial mechanical strain would be exerted on the CH_3-SAM; as a result, overall structure of the CH_3-SAM would be considerably perturbed. In other words, maintaining smooth surface morphology of an AlO_x layer is a key to preserve structural integrities of an underlying SAM; thus, it is not just a coincidence that both the rms roughness of an AlO_x layer is minimized and the structural integrities of an underlying CH_3-SAM layer are well maintained within the narrow window of $R_c \sim 0.2$.

Conclusion

The deposition of AlO_x on strong hydrophobic CH_3-SAM surfaces by two-stage ALD was demonstrated. During a conventional ALD process using water as the oxygen source, the AlO_x layers on the CH_3-SAMs were found to undergo growth instabilities and develop substantially rough surface morphologies, which was attributed to the incomplete surface wetting on the hydrophobic CH_3-SAMs by water in the early stage of the conventional ALD process. In addition, the underlying CH_3-SAMs were found to be significantly disturbed by the conventional ALD process using water. In contrast, the two-stage ALD using *n*-propanol in the first stage improved the surface morphologies of AlO_x noticeably and simultaneously maintained the structural integrities of underlying CH_3-SAMs when R_c was within the narrow window ~0.2, suggesting the importance of explicitly controlling surface wetting in the early stage of an ALD process, in particular, on strong hydrophobic surfaces. The proposed two-stage ALD process successfully demonstrated the deposition of AlO_x on strong hydrophobic CH_3-SAM surfaces by providing smooth surface morphologies of the AlO_x and maintaining structural integrities of the underlying CH_3-SAMs.

CM702848Y

(26) Schlenoff, J. B.; Li, M.; Ly, H. *J. Am. Chem. Soc.* **1995**, *117*, 12528.